

Double stars with wide separations in the AGK3 – I. Components that are themselves spectroscopic binaries

J.-L. Halbwachs,^{1*} M. Mayor² and S. Udry²

¹*Observatoire Astronomique de Strasbourg (UMR 7550), 11 rue de l'Université, F-67 000 Strasbourg, France*

²*Observatoire Astronomique de l'Université de Genève, 51 chemin des maillettes, CH-1290 Sauverny, Switzerland*

Accepted 2011 December 1. Received 2011 November 30; in original form 2011 October 19

ABSTRACT

Wide binaries are tracers of the gravity field of the Galaxy, but their study requires some caution. A large list of common proper motion stars selected from the third Astronomischen Gesellschaft Katalog (AGK3) was monitored with the CORAVEL (for CORrelation RADial VELOCities) spectrovelocimeter, in order to prepare a sample of physical binaries with very wide separations. 66 stars received special attention, since their radial velocities (RV) seemed to be variable. These stars were monitored over several years in order to derive the elements of their spectroscopic orbits. In addition, 10 of them received accurate RV measurements from the SOPHIE spectrograph of the T193 telescope at the Observatory of Haute-Provence.

For deriving the orbital elements of double-lined spectroscopic binaries (SB2), a new method was applied, which assumed that the RV of blended measurements are linear combinations of the RV of the components. 13 SB2 orbits were thus calculated.

The orbital elements were eventually obtained for 52 spectroscopic binaries (SB), two of them making a triple system. 40 SB received their first orbit and the orbital elements were improved for 10 others. In addition, 11 SB were discovered with very long periods for which the orbital parameters were not found. The median period of the 40 first orbits is 1 yr, and several SB should be resolved or should receive an astrometric orbit in future, providing the masses of the components. In addition, it appeared that HD 153252 has a close companion, which is a candidate brown dwarf with a minimum mass of 50 Jupiter masses.

The final selection of wide binaries and the derivation of their statistical properties will be presented in a second paper.

Key words: binaries: spectroscopic – brown dwarfs – stars: low-mass.

1 INTRODUCTION

Binarity is a very common stellar property, which covers a very wide range of separations, from two stellar radii to thousands of astronomical units. Close binaries have short orbital periods (from a few hours to a few years) and they are easily detected from variations in their radial velocities (RV). For that reason, they are the most commonly studied of this class of stars (see e.g. Halbwachs et al. 2003). Binaries with periods of around a few centuries are also rather well-known: the components are sufficiently separated to be detected visually (in the past) or on images and they are still close enough to avoid the risk of confusing a field star and a binary component: the optical companions may be discarded by applying a statistical criterion almost as old as the discovery of double stars (Struve 1852).

Very wide binaries are particularly interesting, since the distribution of their separations is a clue to the gravitational perturbers that made the gravity field of the Galaxy (see Jiang & Tremaine 2010 and references therein). However, the selection of binaries with separations of thousands of astronomical units is difficult: the components also have wide apparent separations and it is necessary to use additional criteria in order to discard the optical companions. Trigonometric parallax, or another estimation of the distance, is sometimes used, but the most efficient and the most employed criterion is proper motion: when the semi-major axis of the orbit is large, the orbital motion of the stars around the barycentre of the system generates a difference in proper motion that is negligible and the components must have similar apparent displacements. Such binaries are called common proper motion (CPM) stars.

In the past, this criterion was used by Luyten to search for wide systems by visual inspection of photographic plates; his investigation was performed over more than 40 years, documented in several papers, from Luyten (1940) to Luyten (1987), and led to the

*E-mail: jean-louis.halbwachs@astro.unistra.fr

discovery of 6121 systems. However, despite their large number, these systems were not used to derive the properties of wide binaries; the main reason is that the selection was based on subjective criteria and, as a consequence, it would be hard to estimate its incompleteness and also contamination by optical pairs. Moreover, since the components of Luyten’s double stars are rather faint (around 16th magnitude), it would be difficult to improve the selection with complementary data.

Another selection of CPM pairs was performed by Halbwachs (1986), on the basis of the new reduction of the second and the third Astronomischen Gesellschaft Katalog (AGK2/3 (Lacroute & Valbousquet 1974). 439 CPM double stars were selected and the number of optical pairs was estimated to be around 40. Since the AGK3 stars are brighter than 12th magnitude, the authors decided to select the physical binaries on the basis of the RV of the components. As is the case for the proper motions, the RV are marginally affected by the orbital motion and the components of wide binaries are therefore also common RV stars. 266 stars were selected and they were measured with the spectrovelocimeter CORAVEL (for CORrelation RADial VELocities). This programme was initiated in 1986 and was initially supposed to end after a few years. However, several stars had variable velocities, since these wide-pair components were themselves spectroscopic binaries (SB). It was then necessary to extend the observations over about 20 years, in order to derive the SB orbital elements and thus the systemic velocity of these stars. The present paper is devoted to these variable velocity stars and to the derivation of their SB elements. The selection of the wide binaries and the derivation of their statistical properties will be treated in a second paper.

The paper is organized as follows: the RV observations are presented in Section 2 and the catalogue of the RV measurements is in Section 3. The calculation of the SB orbits is in Section 4; for the double-lined SB (SB2), we present a method to take into account the measurements related to blends of the two components. Some interesting points relating to the new SB that we have discovered are discussed in the conclusion in Section 5.

2 THE RADIAL VELOCITY MEASUREMENTS

2.1 The CORAVEL observations

The observational programme concerned a large number of the CPM stars listed in Halbwachs (1986). In that paper, the CPM stars were presented in two tables, according to the time $T = \theta/\mu$, where θ is the apparent separation and μ is the proper motion of the pair of stars. 326 pairs of CPM stars with $T < 1000$ years are listed in the first table and the estimated frequency of optical pairs is only 1.3 per cent. The second table contains 113 CPM pairs with T between 1000 and 3500 yr; this range corresponds to an expected frequency of optical pairs of 40 per cent. Since the proportion of optical pairs is rather important in the second table, all these 113 CPM pairs were selected in a first step. For the first table, it was decided to observe only the components of pairs with a primary brighter than 9.15 mag. This limit was chosen since it appeared that the AGK 2/3 is not complete beyond that magnitude.

The spectrovelocimeter CORAVEL (Baranne, Mayor & Poncet 1979) is installed on the Swiss 1-m telescope at the Observatory of Haute-Provence (OHP). For slow rotators with spectral types around K0, it may provide RV measurements with a precision around 0.3 km s^{-1} . However, it becomes inefficient for stars earlier than F5, except when their spectra contain metallic lines. Therefore, it is possible to obtain RV with a precision near 1 km s^{-1} for the

Am-type stars. Due to this restriction, our final programme contains 266 stars observable with CORAVEL: 90 are extracted from the first table and 176 from the second one.

The programme started in 1986, but several stars had already been measured with CORAVEL at this time. The observations of stars with a constant velocity were stopped after 1 or 2 years, but several SB were detected and it was necessary to prolong the programme in order to cover their periods and to derive their orbital elements. In practice, when a SB was observed its wide companion was usually observed too. The CORAVEL observations were performed until the decommissioning of that instrument in 2000. They led to the detection of 66 stars with variable radial velocity, according to the $P(\chi^2)$ test at the 1 per cent threshold.

2.2 The SOPHIE measurements

In 2007, we had the opportunity to obtain very accurate RV measurements with the Spectrographe pour l’Observation des PHénomènes des Intérieurs stellaires et des Exoplanètes (SOPHIE) installed on the 1.93-m telescope at OHP (Perruchot et al. 2008; Bouchy et al. 2009). 10 stars with variable RV, but for which it was still not possible to derive an orbit, were observed in *service mode* during 2 semesters. The spectra were registered in high-resolution mode with a signal-to-noise ratio between 20 and 200, depending on the brightness of the star. Thanks to the SOPHIE automatic pipeline, they were cross-correlated with a mask close to the actual spectral type of the star. For the single-lined binaries (SB1), the RV was directly obtained from the pipeline. For two SB2, the cross-correlation function (CCF) was fitted with two normal distributions in order to derive the velocities of both components.

The automatic pipeline also provides RV uncertainties, but they are obviously underestimated. Boisse et al. (2010) estimate that three terms must be quadratically added: the instrumental drift is around 3 m s^{-1} , the guiding error is around 4 m s^{-1} and they derived from their own observations an additional error of 8 m s^{-1} . We finally obtain an additional error of 9.4 m s^{-1} , which is rounded up to 10 m s^{-1} . It is worth noticing that this error does not apply to the radial velocity with respect to the Sun but to variations of RV due to an exoplanetary companion, i.e. to RV fluctuations over a range not larger than around 100 m s^{-1} . Since we are observing SB with stellar components, the semi-amplitude of the RV is as large as several km s^{-1} and the error could be larger than 10 m s^{-1} . Moreover, we must introduce an offset between the CORAVEL measurements and the SOPHIE measurements. This offset depends on the star and on the mask used in the SOPHIE reduction. It may be computed with the orbital elements when several SOPHIE measurements are available, but for a single measurement it results in an error of 0.3 km s^{-1} , to a rough estimation.

3 THE RV CATALOGUE

In addition to the observations performed with CORAVEL and with SOPHIE, we still obtained three measurements from two other telescopes: the Euler telescope with the CORALIE spectrovelocimeter in La Silla and the 1-m telescope of the Simeis Observatory in Crimea. Finally, 2275 measurements were obtained for the 66 stars that were selected as variable or probably variable. The measurements are gathered in one plain text file, with one header record preceding the RV of each star. Some headers are presented in Table 1. Each header contains the following.

Table 1. Sample of the RV catalogue. The headers of the first six stars; in the catalogue file, each header is immediately followed by N_{meas} measurements. The full catalogue is available as Supporting Information with the electronic version of the article.

CPM	AG	$B - V$	N_{meas}	\bar{V}	$\sigma_{\bar{V}}$	$P(\chi^2)$	Var	α
2 5A	+46 87	0.58	33	-5.484	0.142	0.000	SB2O	00 37
2 5B	+46 86	1.93	19	-15.714	0.370	0.000	VAR	00 37
2 7A	+31 55	0.68	43	-38.802	0.142	0.000	SB1O	00 41
2 8A	-01 87	0.53	51	8.328	0.055	0.000	SB1O	00 58
2 8B	-01 90	0.68	14	10.431	0.195	0.001	SB1	00 58
1 18A	+31 132	0.68	90	17.204	0.075	0.000	SB2O+	01 22

(i) *CPM*, the identification of the star in Halbwachs (1986), which consists of the number of the list followed by the number of the pair, followed by ‘A’ or ‘B’ for the component.

(ii) *AG*, the AG identification.

(iii) $B - V$, the colour index assumed in the derivation of the CORAVEL radial velocities.

(iv) N_{rec} , the number of measurements following the header.

(v) \bar{V} , the mean radial velocity of the star. When a spectroscopic orbit was derived, as indicated by ‘O’ in the variability status, \bar{V} is the velocity of the system. Otherwise, it is an average of the CORAVEL measurements with a zero or a blank in the ‘c’ column of Table 2, as explained in Section 4.3.

(vi) $\sigma_{\bar{V}}$, the uncertainty in \bar{V} .

(vii) $P(\chi^2)$, the probability of obtaining a χ^2 larger than the one actually obtained, assuming the RV is constant in reality. The χ^2 was computed from the CORAVEL measurements of the primary component.

(viii) The final variability status of the star. The following were used: ‘CST?’ for a star that could have a constant RV, ‘VAR’ when the RV seems to be variable, ‘SB1’ or ‘SB2’ when at least part of the velocity curve is visible, ‘SB1O’ and ‘SB2O’ when the orbital elements were derived.

(ix) A ‘+’ follows the variability status SB1O or SB2O when RV measurements from an external source were taken into account to derive the orbital elements. These additional measurements were found in the SB9 online catalogue (Pourbaix et al. 2004); they are not reproduced here, but the references are given in the notes in Section 4.4.

(x) The right ascension of the ‘A’ component, in hours and minutes, is given in order to facilitate searches for the stars.

The headers are followed by the measurement records (Table 2), which consist of the following.

(i) The epoch of the observation, in barycentric Julian days, counted since JD 240 0000. The decimal part is restricted to 3 digits for the CORAVEL measurements but 4 digits for the SOPHIE measurements.

(ii) V_R , the RV in km s^{-1} . The last digit corresponds to 10 m s^{-1} for the CORAVEL measurements but to 1 m s^{-1} for the SOPHIE measurements. As often as possible, the SOPHIE measurements were corrected for a systematic shift between them and the CORAVEL ones; the correction is then indicated in the notes in Section 4.4.

(iii) σ_{RV} , the uncertainty of V_R , in km s^{-1} , with the same number of digits as V_R .

(iv) *c*, an index indicating the measured component of the SB2: ‘1’ for the primary, ‘2’ for the secondary and ‘0’ for a blend of both components; blank for SB1.

Table 2. Sample of the RV catalogue. Some measurements following the headers of two of the stars, a SB1 and a SB2. The full catalogue is available as Supporting Information with the electronic version of the article.

JD	V_R	σ_{RV}	<i>c</i>	<i>f</i>	<i>T</i>
+2 400 000	km s^{-1}	km s^{-1}			
48053.561	-16.57	0.31		R	C
48139.335	-17.65	0.36			C
48878.544	-18.62	0.30			C
49083.925	-17.77	0.32			C
54214.6265	-17.568	0.010			S
54255.5037	-17.551	0.010			S
50548.336	-10.58	0.41	0		C
50819.550	-12.44	0.35	0		C
51197.532	-17.86	0.53	1		C
51197.532	-4.52	1.07	2		C
51519.512	-15.35	0.32	1		T
51616.605	8.56	0.05	1		E

(v) *f*, a flag coded as follows: ‘R’ when the measurement was rejected in the final calculation and ‘F’ when it applies to a component with a fixed velocity.

(vi) *T*, a flag indicating the telescope used for the measurement: ‘C’= 1 m/CORAVEL telescope in Haute-Provence (2208 occurrences), ‘E’= Euler/CORALIE telescope at La Silla, Chile (2 occurrences), ‘S’= T193/SOPHIE (62 occurrences) and ‘T’= 1-m telescope of the Simeis Observatory in Crimea (1 measurement).

Some of the header data are included in Table 3, where the statistical indicators of variability are also presented. The full RV catalogue is available as Supporting Information with the electronic version of the article.

4 CALCULATION OF THE SB ORBITS

4.1 Orbits with ‘blended’ measurements

The calculation of the orbital elements of the SB2 systems requires one to answer the preliminary question: what can we do when the RV of the components are close to the systemic velocity and when only one RV is obtained from the CCF since only one dip is visible? A solution is to fit the CCF with two Gaussian curves, assuming the widths and the depth ratio of the CCF components from the observations where they are well separated (Duquenois 1987). However, the RV then obtained are not very reliable in practice. Our idea is then to keep the blended measurements as they are and to use a simple model to express them as a function of the RV of

Table 3. The average velocities of the stars classified as variable on the basis of $P(\chi^2) < 1$ per cent. N_{CORA} is the number of CORAVEL observations and ΔT_{CORA} is the time-span of these observations. The three columns that follow are statistical quantities referring to these N_{CORA} measurements of the primary component or of blends: I is their ‘internal’ error, i.e. an estimation of the average σ_{RV} derived from the mean of the weights, E/I is the external-to-internal error ratio, where E is the standard deviation of V_R , and $P(\chi^2)$ is the probability of obtaining such a large value of E/I when the RV of the star is constant in reality. ΔT_{meas} is the time-span of all observations when other sources are added; N_{meas} is the total number of RV measurements (all sources and all components); for readability, N_{meas} and ΔT_{meas} are given only when they are different from N_{CORA} or ΔT_{CORA} , respectively. An asterisk indicates when the SB orbit is the first for this object and \bar{V} is the velocity of the system in km s^{-1} .

CPM	HD/BD/HIP	RA	N_{CORA}	ΔT_{CORA}	I	E/I	$P(\chi^2)$	N_{meas}	ΔT_{meas}	Var	1st orbit	\bar{V}
2: 5A	BD +45 172	00 37	21	4160	0.456	7.40	0.000	33	7481	SB2O	*	-5.484 ± 0.142
2: 5B	BD +45 171	00 37	19	4160	0.606	2.66	0.000			VAR		-15.714 ± 1.568
2: 7A	HD 4153	00 41	43	4396	0.350	32.92	0.000			SB1O	*	-38.802 ± 0.142
2: 8A	HD 5947	00 58	51	4461	0.445	17.38	0.000			SB1O	*	8.328 ± 0.055
2: 8B	BD -01 133	00 58	11	4316	0.379	1.70	0.001	14	7729	SB1		10.431 ± 0.615
1: 18A	HD 8624	01 22	47	3291	0.473	80.14	0.000	90		SB2O		17.204 ± 0.075
1: 19B	HD 8956	01 25	60	7371	0.580	31.98	0.000	100		SB2O	*	4.739 ± 0.108
2: 13A	BD +10 303	02 13	14	4158	0.501	4.58	0.000			SB1O	*	-0.911 ± 0.255
2: 14A	HD 13904	02 13	10	4158	0.486	2.32	0.000	16	7443	SB1		-2.457 ± 1.070
1: 31B	BD +57 530	02 13	26	3735	0.427	7.26	0.000			SB1O	*	11.923 ± 0.084
2: 15A	BD +28 387s	02 16	11	4466	0.460	2.19	0.000	14	7703	SB1		8.595 ± 0.961
2: 15B	BD +28 387	02 16	30	4466	0.507	29.24	0.000	36		SB2O	*	-6.766 ± 0.323
2: 16A	HD 14446	02 17	32	4462	1.813	14.29	0.000	38	7634	SB2O	*	-5.765 ± 1.843
2: 19B	BD +22 353	02 26	22	4462	0.564	4.61	0.000			SB1O	*	19.295 ± 0.100
2: 20B	BD +17 493p	03 04	22	4469	0.997	43.38	0.000	39		SB2O	*	-13.415 ± 0.197
2: 21B	BD +20 511	03 06	32	4472	1.682	1.64	0.000	37	7764	SB1		25.270 ± 2.718
2: 24B	HD 23158	03 40	5	1601	2.711	2.38	0.000			VAR?		-0.083 ± 5.770
2: 33A	HD 27635	04 21	26	4464	0.404	9.83	0.000	34		SB1O	*	-39.512 ± 0.188
2: 33B	BD +63 499	04 21	22	4372	0.366	17.39	0.000			SB1O	*	-38.551 ± 0.137
2: 38B	HD 285970	04 39	30	3735	0.390	51.60	0.000	33		SB2O		13.663 ± 0.172
2: 40A	HD 33185	05 06	23	4471	0.436	4.95	0.000	31		SB2O	*	-3.982 ± 0.214
2: 41B	HD 241105	05 06	16	3664	0.423	10.98	0.000			SB1O	*	16.073 ± 0.068
2: 48B	HD 59450	07 27	20	7286	0.409	6.47	0.000			SB1O	*	-2.379 ± 0.094
1: 90A	HD 69894	08 17	3	449	0.455	2.46	0.003			VAR		0.016 ± 0.912
1: 93A	HD 71149	08 23	26	3668	0.464	21.73	0.000	44	4087	SB2O	*	-11.329 ± 0.093
2: 54B	HD 80101a	09 15	39	3668	0.512	19.05	0.000	48		SB2O	*	55.561 ± 0.172
1:112A	HD 81997	09 26	52	6541	1.044	2.35	0.000			SB1O		10.484 ± 0.190
1:114A	BD +15 2080	09 33	32	3664	0.389	8.74	0.000			SB1O	*	-4.562 ± 0.077
2: 58A	HD 89730	10 18	31	3989	1.149	7.56	0.000			SB1O	*	18.837 ± 0.243
2: 58B	HD 89745	10 18	27	3989	1.067	3.77	0.000	44	7283	SB2O	*	18.463 ± 0.302
1:130A	HD 92787	10 40	11	2970	3.272	3.58	0.000	12		SB2		4.962 ± 5.341
1:130B	HD 92855	10 40	47	3221	0.447	32.96	0.000			SB1O		4.092 ± 0.087
1:141A	HD 97815	11 12	34	3669	0.324	36.60	0.000			SB1O	*	-11.329 ± 0.065
2: 62A	HD 98528	11 17	4	771	0.305	2.94	0.000			VAR		-11.135 ± 0.777
2: 64B	HD 100267	11 29	34	4380	1.908	31.48	0.000			SB1O		13.143 ± 0.912
2: 65B	BD +42 2231	11 36	26	3993	0.417	10.66	0.000			SB1O	*	12.415 ± 0.069
1:156A	HD 102509	11 45	12	5522	0.451	55.54	0.000			SB2O		0.750 ± 0.050
1:156B	BD +21 2357	11 45	9	3665	0.429	2.51	0.000			SB1		2.855 ± 1.017
2: 68B	BD +28 2103	12 16	40	3890	0.362	9.85	0.000			SB1O		17.970 ± 0.065
2: 70A	HD 109509	12 32	17	5846	0.493	5.72	0.000			SB1O	*	-17.949 ± 0.114
2: 72A	HD 110025	12 36	43	5462	0.530	42.10	0.000			SB1O	*	-1.680 ± 0.112
2: 72B	BD +17 2512	12 36	34	4380	0.421	12.38	0.000			SB1O	*	-16.052 ± 0.105
2: 73B	HD 110106	12 36	22	3884	0.366	10.10	0.000			SB1O	*	-8.555 ± 0.087
2: 74B	BD +26 2401	12 49	37	3894	0.483	26.67	0.000	50		SB2O	*	-4.004 ± 0.122
1:175A	HD 112033	12 50	26	7943	0.299	5.48	0.000	33	11270	SB1O	*	-6.091 ± 0.075
2: 78A	HD 117044	13 25	45	3909	1.603	2.69	0.000			SB1O	*	-12.078 ± 1.735
2: 79B	HD 117433	13 26	49	4377	0.631	18.69	0.000	79		SB2O	*	-9.784 ± 0.164
2: 81B	HD 234054	13 35	23	3985	0.330	5.53	0.000			SB1		-43.600 ± 1.784
2: 83B	BD +37 2460	13 50	23	4255	0.391	7.29	0.000			SB1O	*	10.150 ± 0.071
2: 84B	BD +40 2713	13 58	29	3701	0.430	40.25	0.000			SB1O	*	-14.058 ± 0.073
2: 85B	HIP 69885	14 16	18	3954	0.444	9.42	0.000	20		SB2O	*	2.924 ± 0.235
2: 87A	HD 126661	14 24	36	7002	1.425	2.95	0.000	43		SB2		-27.832 ± 2.029
2: 89A	HD 135117	15 03	22	4160	0.476	5.71	0.000	26	7305	SB1		2.026 ± 2.657
2: 91B	HD 150631	16 37	12	2961	2.761	2.08	0.000			VAR?		-12.958 ± 5.490
2: 92A	HD 153252	16 55	34	4004	0.569	8.30	0.000			SB1O	*	-77.890 ± 0.147
1:246B	HD 160010	17 14	41	3744	0.635	60.52	0.000	45		SB2O	*	6.995 ± 0.115
2: 94A	HD 158916	17 28	35	4112	0.648	7.06	0.000			SB1O	*	-22.512 ± 0.127

Table 3 – *continued*

CPM	HD/BD/HIP	RA	N_{CORA}	ΔT_{CORA}	I	E/I	$P(\chi^2)$	N_{meas}	ΔT_{meas}	Var	1st orbit	\bar{V}
2: 97B	HD 164025	17 55	39	4103	0.528	80.98	0.000			SB1O		-24.130 ± 0.060
1:258A	HD 167215	18 11	22	7010	0.440	3.15	0.000			SB1O	*	-42.805 ± 0.075
2: 98B	HD 238865	18 23	50	4037	0.719	33.70	0.000			SB1O		-23.459 ± 0.227
2: 99A	HD 169822	18 23	16	4452	0.343	2.73	0.000			SB1O		-18.977 ± 0.101
2: 99B	HD 169889	18 23	10	2153	0.336	1.84	0.000	21	7406	CST?		-17.952 ± 0.587
1:280A	HD 194765	20 24	41	2963	0.584	21.04	0.000	72		SB2O	*	-15.255 ± 0.081
1:300B	BD +17 4697p	22 06	46	3764	0.643	62.47	0.000	90		SB2O	*	20.963 ± 0.121
1:307A	HD 214511	22 34	52	3763	0.850	35.57	0.000	80		SB2O		-4.756 ± 0.415
2:109B	BD +08 4904	22 35	43	4400	0.622	35.32	0.000			SB1O	*	-29.873 ± 0.114

the components; the orbital elements are then derived from all the measurements.

When C is the relative contribution of the primary velocity, V_1 , to the measured velocity, V_0 , we have the relation

$$V_0 = C V_1 + (1 - C) V_2, \quad (1)$$

where V_2 is the RV of the secondary component. The radial velocities obtained with CORAVEL and with SOPHIE are derived by fitting the CCF with a background level minus a normal distribution (Baranne et al. 1979). When the standard deviations and the depths of the CCF of the components are fixed, C is a function of $\Delta V_R = |V_1 - V_2|$. In order to see the shape of that function, we consider a simple example hereafter: the same standard deviation, σ_{CCF} , is assumed for both correlation dips, and we apply several depth ratios d_2/d_1 . We calculate the sum of two normal distributions and the position of the blend, V_0 , is derived by fitting to the sum a single normal distribution. The value of C is then derived by inverting equation (1). These operations are repeated for several separations between the centres of the two correlation dips, as long as the blended distribution exhibits a sole minimum. The results are represented in Fig. 1. Each line corresponds to a fixed depth ratio, which is $d_2/d_1 = (1 - C(0))/C(0)$, where $C(0)$ is the value of C when the velocities of the components are nearly the same ('nearly' but not exactly: it is not possible to derive C when the two dips are perfectly superposed).

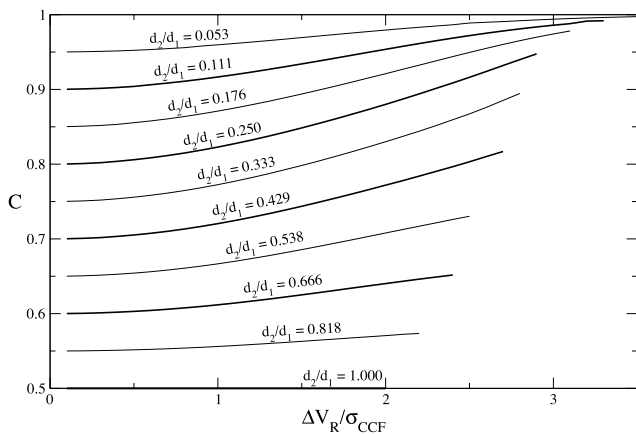


Figure 1. Simulation of the velocity of a blended measurement with respect to the difference of radial velocity between the components. C is the relative contribution of the primary velocity, V_1 , to the measured velocity of the blended CCF, V_0 . Each line refers to a couple of correlation dips with the same standard deviation, σ_{CCF} , and with fixed depth ratio d_2/d_1 . The end of the line corresponds to the appearance of two minima in the blended dip. ΔV_R is the absolute value of the difference between the component velocities, $|V_1 - V_2|$.

It appears from Fig. 1 that C could be represented by a polynomial with terms less and less significant when the order increases: the most important is C_0 and a slope may possibly be added, since C may be as large as $C_0 + 0.1$ when $|V_1 - V_2|$ is large. Then $C = C_0 + C_1|V_1 - V_2|$. The (C_0, C_1) coefficients were calculated as terms of the orbital solution for 7 of the 8 systems with more than 10 blended measurements, which are presented in Fig. 2 (the triple system 2:54B was set aside). It appeared that C_1 was never significant, since its maximum value, which was obtained for system 2:74B, was only 2.35 times its uncertainty. Moreover, negative values were found for three systems (1:19B, 2:58B and 2:79B), although this should not happen in theory. We conclude therefore that the C_0 term is sufficient for deriving the blended velocities. This is easily confirmed by a visual inspection of Fig. 2, where the model velocity curves derived by assuming only the C_0 term in the expression of C are represented. The blended measurements are equally distributed around the theoretical curves and no deviation related to $|V_1 - V_2|$ is visible in practice.

4.2 The orbits

It was possible to derive the orbital elements for 51 stars, including a triple-system solution that consists of two orbits. The spectroscopic orbits are presented in Tables 4–6. We count 40 first orbits: 27 SB1 and 13 SB2. The 12 other orbits are distributed as follows. Six are new orbits that were computed taking into account other measurements in addition to ours; these calculations were done including the offset between the 2 RV sources as a free parameter of the model. Two other orbits are published orbits that were partly based on our measurements; they are just expressed with the same conventions as the others, RV in the CORAVEL system and epochs in Julian days. The last four orbits are new orbits derived from our measurements alone, since including the others did not ameliorate the solution.

The phase plots of 49 orbits are available in electronic form (see Supporting Information). The two orbits that were already published are not drawn again.

4.3 The SB without orbits

In Table 3, we count 15 stars for which it was not possible to derive a spectroscopic orbit. In addition, we still found two triple systems (2:16A and 2:98B) with a short-period SB and a drift in the residual RV. The figures showing the radial velocities of these 17 stars as functions of the epochs are given in electronic form (see Supporting Information). In addition to the two triple systems already mentioned, we still count seven long-period SB1 (2:8B, 2:14A,

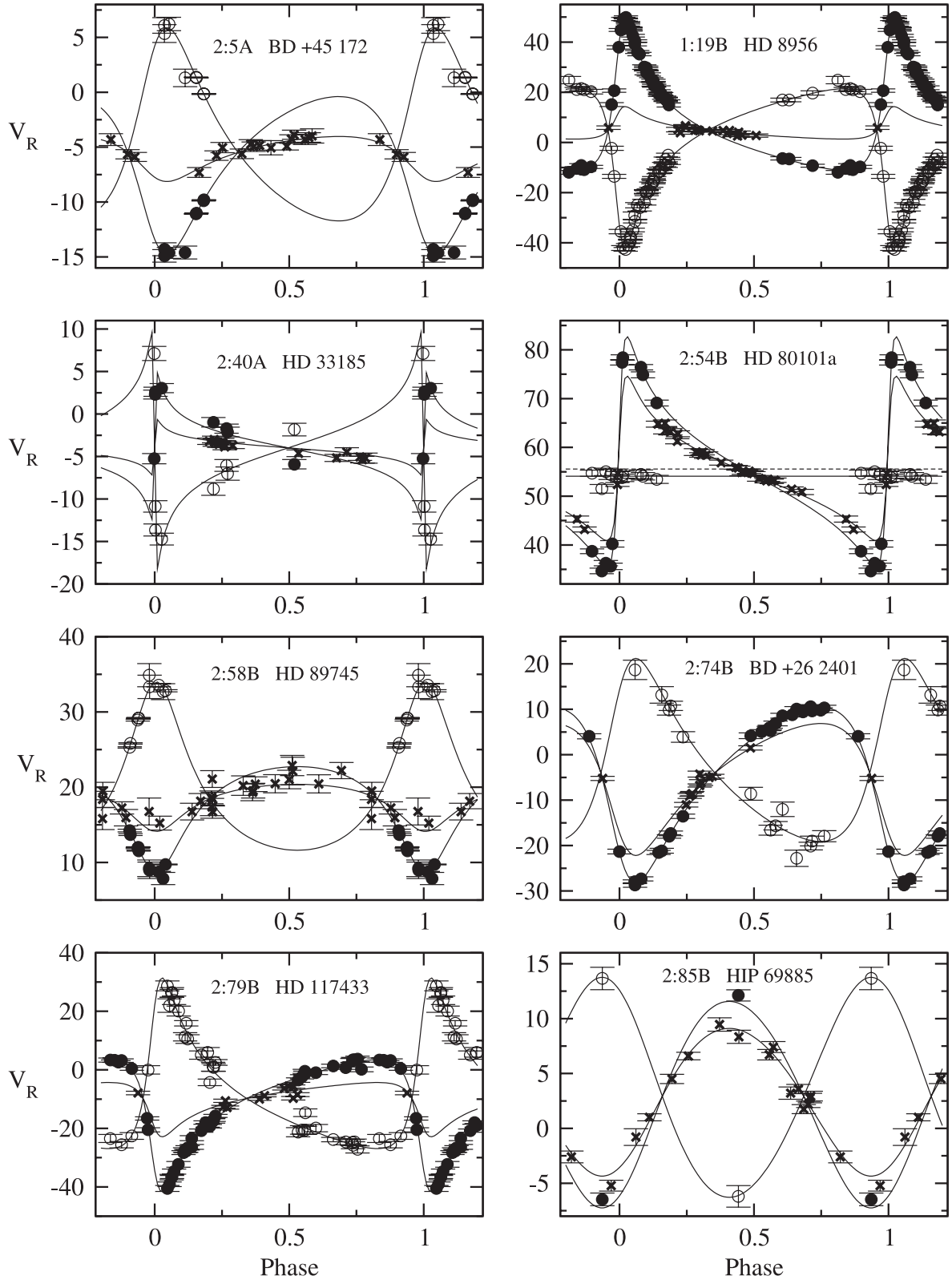


Figure 2. The orbits of SB2 with at least 10 blended RV measurements, assuming the blends are linear combinations of the primary and secondary velocity. The black discs are the RV of the primary component, the circles refer to the secondary component and the crosses to the measurements obtained from blended CCF peaks. The solid lines refer to the orbital elements. The system 2:54B is triple and the secondary is in reality a long-period component of a close SB1; the RV of the secondary is then fixed; the dashed line is the barycentric velocity of the close binary. The triple system 1:307A is not represented here, since the blended RV are then combinations of the primary RV of a short-period SB1 and a secondary RV with a period much longer; therefore, it is not possible to fold them in phase.

Table 4. The orbital elements of the SB up to RA = 9^h30. The numbers of measurements refer to our measurements listed in the RV catalogue presented in Section 3 plus, where available, measurements from external sources. An asterisk following the CPM name refers to a remark in Section 4.4.

HD/BD/HIP CPM	P (d)	T_0 (JD) 2400000+	e	V_0 (km s ⁻¹)	ω_1 (°)	$K_{1,2}$ (km s ⁻¹)	$m_{1,2} \sin^3 i$ or $f_1(m)$ (M _☉)	$a_{1,2} \sin i$ (Gm)	$N_{1,2}$ N_0	$\sigma(O - C)$ (km s ⁻¹)	C_0
BD +45 172 2:5A*	5556. ±79.	47941. ±69.	0.359 ±0.069	-5.484 ±0.142	144.21 ±3.11	7.18 ±0.40	1.05 ±0.23	512. ±35.	8	0.586	0.679 ±0.033
						8.80 ±0.49	0.86 ±0.19	628. ±43.	8 17		
HD 4153 2:7A	25.06543 ±0.00118	49976.293 ±0.054	0.5642 ±0.0089	-38.802 ±0.142	78.45 ±1.38	19.059 ±0.238	0.01014 ±0.00044	5.4238 ±0.0788	43	0.827	
HD 5947 2:8A	58.56668 ±0.00505	47871.527 ±0.245	0.4022 ±0.0060	8.328 ±0.055	96.21 ±1.27	10.420 ±0.075	0.00528 ±0.00012	7.6826 ±0.0594	51	0.336	
HD 8624 1:18A*	14.908342 ±0.000049	49000.156 ±0.025	0.1342 ±0.0015	17.204 ±0.075	26.39 ±0.60	54.375 ±0.111	0.9736 ±0.0047	11.046 ±0.022	44+17	0.616	0.564 ±0.035
						54.573 ±0.121	0.9700 ±0.0045	11.086 ±0.024	43+15 3+0		
HD 8956 1:19B	115.6041 ±0.0040	47976.745 ±0.105	0.6543 ±0.0037	4.739 ±0.108	316.71 ±0.64	30.170 ±0.190	0.6308 ±0.0100	36.267 ±0.213	44	1.011	0.618 ±0.018
						31.756 ±0.254	0.5993 ±0.0082	38.174 ±0.282	40 16		
BD +10 303 2:13A*	5231. ±747.	47578. ±90.	0.73 ±0.33	-0.911 ±0.255	243. ±16.	4.052 ±0.621	0.0115 ±0.0056	199.2 ±41.7	14	0.494	
BD +57 530 1:31B	1678. ±15.	46663. ±31.	0.523 ±0.015	11.923 ±0.084	243.1 ±2.8	4.66 ±0.10	0.01094 ±0.00080	91.7 ±2.4	26	0.297	
BD +28 387 2:15B	41.2013 ±0.0033	49925.062 ±0.287	0.3681 ±0.0146	-6.766 ±0.323	9.87 ±1.18	23.672 ±0.494	0.2246 ±0.0197	12.470 ±0.271	30	1.693	
						26.23 ±1.27	0.2027 ±0.0154	13.815 ±0.675	6		
HD 14446 2:16A*	9.17583 ±0.00064	49982.64 ±0.58	0.154 ±0.076	-5.76 ±1.84	263.8 ±24.9	36.11 ±2.26	0.0421 ±0.0083	4.502 ±0.287	25	7.85	
BD +22 353 2:19B	276.426 ±0.362	47410.72 ±6.45	0.277 ±0.035	19.295 ±0.100	186.74 ±8.66	3.744 ±0.143	0.001336 ±0.000159	13.67 ±0.54	22	0.432	
BD +17 493p 2:20B*	11.962591 ±0.000064	49995.0938 ±0.0167	0.3965 ±0.0035	-13.415 ±0.197	252.67 ±0.67	64.974 ±0.331	1.1671 ±0.0151	9.8122 ±0.0523	18	1.059	
						68.330 ±0.377	1.1098 ±0.0142	10.3189 ±0.0594	17		
HD 27635 2:33A*	68.3447 ±0.0159	47817.24 ±0.98	0.485 ±0.035	-39.512 ±0.188	180.5 ±6.9	5.948 ±0.293	0.000998 ±0.000162	4.887 ±0.264	26	0.861	
BD +63 499 2:33B	2630.26 ±9.97	50113.80 ±1.33	0.9125 ±0.0031	-38.551 ±0.137	242.23 ±2.67	14.064 ±0.543	0.0520 ±0.0059	208.13 ±7.90	22	0.508	
HD 285970 2:38B*	56.44579 ±0.00357	49965.668 ±0.217	0.3627 ±0.0075	13.663 ±0.172	190.88 ±1.58	26.397 ±0.174	0.6404 ±0.0248	19.093 ±0.139	30	0.697	
						35.379 ±0.771	0.4778 ±0.0156	25.590 ±0.564	3		
HD 33185 2:40A*	1469.41 ±0.58	49346.79 ±3.95	0.9021 ±0.0090	-3.982 ±0.214	271.6 ±17.1	8.65 ±1.21	0.087 ±0.036	44.51 ±4.01	8	1.160	0.762 ±0.061
						13.95 ±1.65	0.054 ±0.023	60.83 ±4.96	8 15		
HD 241105 2:41B	2273.8 ±10.2	47555.2 ±11.3	0.4731 ±0.0214	16.073 ±0.068	263.14 ±2.67	7.939 ±0.235	0.0808 ±0.0079	218.68 ±7.15	16	0.182	
HD 59450 2:48B*=2:49A	2708.2 ±32.9	44826.2 ±28.3	0.716 ±0.098	-2.379 ±0.094	263.19 ±5.24	4.93 ±1.07	0.0115 ±0.0090	128.2 ±33.5	20	0.337	
HD 71149 1:93A	1498.3 ±2.6	48593.4 ±2.2	0.6876 ±0.0043	-11.329 ±0.093	308.84 ±1.23	13.985 ±0.094	0.8905 ±0.0305	209.20 ±2.23	23	0.612	0.683 ±0.032
						16.320 ±0.154	0.7631 ±0.0236	244.12 ±3.35	16 5		
HD 80101 2:54B*	52.81576 ±0.00077	49906.629 ±0.047	0.7522 ±0.0049	55.561 ±0.172	281.90 ±1.27	23.53 ±0.32	0.02041 ±0.00077	11.262 ±0.182	10	0.890	0.717 ±0.023
HD 81997 1:112A*	2815. ±46.	47994. ±87.	0.427 ±0.092	10.484 ±0.190	332.7 ±16.8	2.79 ±0.31	0.00469 ±0.00173	97.7 ±12.1	52	1.217	

Table 5. Same as Table 4, for SB with RA between $9^{\text{h}}30$ and $17^{\text{h}}15$.

HD/BD/HIP CPM	P (d)	T_0 (JD) 2400000+	e	V_0 (km s $^{-1}$)	ω_1 ($^\circ$)	$K_{1,2}$ (km s $^{-1}$)	$m_{1,2} \sin^3 i$ or $f_1(m)$ (M_\odot)	$a_{1,2} \sin i$ (Gm)	$N_{1,2}$ N_0	$\sigma(O - C)$ (km s $^{-1}$)	C_0
BD +15 2080 1:114A	383.78 ± 0.36	48194.7 ± 5.8	0.1920 ± 0.0145	-4.562 ± 0.077	10.31 ± 5.69	5.141 ± 0.100	0.00511 ± 0.00030	26.62 ± 0.52	32	0.296	
HD 89730 2:58A	61.9981 ± 0.0168	49934.68 ± 0.39	0.623 ± 0.032	18.837 ± 0.243	201.43 ± 3.16	15.027 ± 0.858	0.01045 ± 0.00209	10.02 ± 0.66	31	1.174	
HD 89745 2:58B*	2303.6 ± 10.5	49789.4 ± 26.8	0.3902 ± 0.0176	18.463 ± 0.302	174.8 ± 4.8	6.983 ± 0.183	0.6876 ± 0.0299	203.6 ± 6.3	10	1.081	0.788 ± 0.037
						11.184 ± 0.197	0.4293 ± 0.0224	326.2 ± 6.6	10 24		
HD 92855 1:130B*	5.6179028 ± 0.0000175	49997.0514 ± 0.0114	0.3203 ± 0.0041	4.092 ± 0.087	104.62 ± 0.86	21.652 ± 0.098	0.005022 ± 0.000070	1.5844 ± 0.0074	47+26	0.881	
HD 97815 1:141A	86.6079 ± 0.0047	49954.45 ± 0.33	0.1966 ± 0.0050	-11.329 ± 0.065	236.4 ± 1.5	17.172 ± 0.089	0.04293 ± 0.00068	20.05 ± 0.11	34	0.339	
BD +12 2343 2:64B*	0.786149 ± 0.000001	49053.871 ± 0.076	0.023 ± 0.014	13.14 ± 0.91	296. $\pm 35.$	90.36 ± 1.32	0.0602 ± 0.0026	0.9766 ± 0.0143	34	5.019	
BD +42 2231 2:65B	951.52 ± 2.14	46738.7 ± 92.7	0.0279 ± 0.0154	12.415 ± 0.069	186.5 ± 35.3	6.197 ± 0.099	0.02349 ± 0.00112	81.06 ± 1.30	26	0.348	
HD 102509 1:156A*	71.6906 ± 0.0004	48431.41 ± 0.03	0 fixed	0.75 ± 0.05	0 ± 0	30.12 ± 0.07	0.980 ± 0.086	29.69 ± 0.07	12+127		
						33.0 ± 1.4	0.895 ± 0.04	32.5 ± 1.4	0+23		
BD +28 2103 2:68B*	2242.3 ± 18.2	50107.0 ± 9.3	0.4402 ± 0.0118	17.970 ± 0.065	294.25 ± 2.38	4.808 ± 0.070	0.01870 ± 0.00086	133.11 ± 2.19	40+52	0.498	
HD 109509 2:70A	4091.2 ± 51.6	43192. $\pm 385.$	0.0736 ± 0.0272	-17.949 ± 0.114	350. $\pm 33.$	4.019 ± 0.166	0.02735 ± 0.00342	225.46 ± 9.77	17	0.317	
HD 110025 2:72A*	54.87832 ± 0.00140	49945.910 ± 0.100	0.3469 ± 0.0045	-1.680 ± 0.112	184.17 ± 0.80	30.703 ± 0.138	0.1361 ± 0.0029	21.730 ± 0.105	43	0.622	
BD +17 2512 2:72B*	595.37 ± 1.00	49460.66 ± 4.61	0.3548 ± 0.0158	-16.052 ± 0.105	58.71 ± 3.50	8.223 ± 0.168	0.02810 ± 0.00180	62.94 ± 1.35	34	0.522	
HD 110106 2:73B*	2899.2 ± 20.5	46789.4 ± 33.7	0.2600 ± 0.0172	-8.555 ± 0.087	129.90 ± 3.84	6.821 ± 0.152	0.0860 ± 0.0059	262.59 ± 6.26	22	0.336	
BD +26 2401 2:74B	19.43553 ± 0.00100	49241.235 ± 0.110	0.3832 ± 0.0100	-4.004 ± 0.122	130.95 ± 1.93	19.302 ± 0.193	0.0499 ± 0.0034	4.764 ± 0.042	26	1.300	0.879 ± 0.026
						20.17 ± 0.69	0.0477 ± 0.0018	4.979 ± 0.164	13 11		
HD 112033 1:175A*	2908.25 ± 4.27	51417.2 ± 4.4	0.6305 ± 0.0073	-6.091 ± 0.075	347.48 ± 0.32	5.455 ± 0.067	0.02287 ± 0.00109	169.31 ± 3.33	33	0.291	
HD 117044 2:78A	1894.3 ± 18.4	46670.3 ± 30.1	0.669 ± 0.149	-12.08 ± 1.74	8.51 ± 7.63	20.0 ± 14.4	0.64 ± 1.43	386. $\pm 287.$	45	1.76	
HD 117433 2:79B	120.0270 ± 0.0137	49437.650 ± 0.226	0.6086 ± 0.0153	-9.784 ± 0.164	132.70 ± 1.36	22.586 ± 0.687	0.486 ± 0.031	29.58 ± 0.56	38	1.68	0.743 ± 0.028
						29.17 ± 1.04	0.376 ± 0.020	38.20 ± 0.99	30 11		
BD +37 2460 2:83B	1235.95 ± 3.38	49480.74 ± 7.15	0.4368 ± 0.0210	10.150 ± 0.071	306.63 ± 3.03	4.335 ± 0.105	0.00761 ± 0.00061	66.27 ± 1.78	23	0.318	
BD +40 2713 2:84B	13.880363 ± 0.000064	47969.8906 ± 0.0293	0.2515 ± 0.0038	-14.058 ± 0.073	100.86 ± 0.91	27.735 ± 0.119	0.02788 ± 0.00037	5.1236 ± 0.0225	29	0.370	
HIP 69885 2:85B	912.61 ± 4.57	49402. $\pm 85.$	0.092 ± 0.039	2.924 ± 0.235	208. $\pm 33.$	9.41 ± 0.74	0.353 ± 0.100	117.6 ± 9.2	2	0.710	0.862 ± 0.041
						10.02 ± 1.33	0.332 ± 0.069	125.2 ± 16.7	2 16		
HD 153252 2:92A*	5.526174 ± 0.000142	47991.656 ± 0.751	0.0302 ± 0.0320	-77.890 ± 0.147	307.3 ± 48.3	6.547 ± 0.165	0.0001609 ± 0.0000121	0.4973 ± 0.0125	34	0.681	
HD 160010 1:246B	5.922546 ± 0.000019	49998.328 ± 0.096	0.0295 ± 0.0029	6.99 ± 0.12	272.3 ± 5.9	53.13 ± 0.16	0.934 ± 0.017	4.325 ± 0.013	41	0.727	
						82.59 ± 0.86	0.6011 ± 0.0091	6.723 ± 0.070	4		

Table 6. Same as Table 4, for SB with RA beyond 17^h15.

HD/BD/HIP CPM	P (d)	T_0 (JD) 2400000+	e	V_0 (km s ⁻¹)	ω_1 (°)	$K_{1,2}$ (km s ⁻¹)	$m_{1,2} \sin^3 i$ or $f_1(m)$ (M_\odot)	$a_{1,2} \sin i$ (Gm)	$N_{1,2}$ N_0	$\sigma(O - C)$ (km s ⁻¹)	C_0
HD 158916 2:94A	941.43 ±2.18	48155.00 ±4.86	0.5345 ±0.0221	-22.512 ±0.127	99.84 ±3.13	6.091 ±0.151	0.01334 ±0.00119	66.65 ±1.99	35	0.644	
HD 164025 2:97B*	3.6550085 ±0.0000015	51089.834 ±0.025	0.0334 ±0.0014	-24.13 ±0.06	148.8 ±2.5	57.64 ±0.08	0.07256 ±0.00032	2.895 ±0.004	39+55	0.53	
HD 167215 1:258A	3518. ±79.	48241. ±18.	0.666 ±0.056	-42.805 ±0.075	167.2 ±4.5	2.64 ±0.32	0.0028 ±0.0012	95. ±13.	22	0.337	
HD 238865 2:98B*	2.709621 ±0.000017	49997.2337 ±0.1515	0.0171 ±0.0065	-23.459 ±0.227	297. ±20.	34.48 ±0.21	0.011503 ±0.000214	1.2845 ±0.0080	29+16	1.005	
HD 169822 2:99A*	293.35 ±0.41	49864.7 ±3.9	0.586 ±0.062	-18.977 ±0.101	166.4 ±8.4	1.079 ±0.095	0.000020 ±0.000005	3.52 ±0.27	16+58	0.422	
HD 194765 1:280A*	160.831 ±0.057	49251.80 ±0.82	0.2536 ±0.0071	-15.255 ±0.081	106.5 ±1.8	16.303 ±0.128 19.297 ±0.211	0.3688 ±0.0086 0.3116 ±0.0059	34.87 ±0.26 41.28 ±0.43	36 31 5	0.769	0.683 ±0.024
BD +17 4697p 1:300B	9.287228 ±0.000040	50000.650 ±0.025	0.1812 ±0.0028	20.96 ±0.12	337.11 ±1.04	55.60 ±0.21 59.60 ±0.25	0.7236 ±0.0068 0.6750 ±0.0058	6.982 ±0.026 7.484 ±0.032	44 44 2	1.079	0.736 ±0.061
HD 214511AB 1:307A*	18504. fixed	49521. ±42.	0.775 ±0.026	-4.76 ±0.42	169.3 ±3.6	6.28 ±0.55 11.10 ±0.55	1.624 ±0.255 0.918 ±0.128	1010. ±71. 1786. ±122.	33 28 19	1.676	0.928 ±0.022
HD 214511A 1:307A*	4.570605 ±0.000023	49980.9590 ±0.0069	0.00 fixed	-	-	46.49 ±0.29	0.04756 ±0.00088	2.921 ±0.018	33	1.015	
BD +08 4904 2:109B	7.644897 ±0.000036	47995.0000 ±0.0819	0.0742 ±0.0055	-29.873 ±0.114	303.69 ±3.90	30.909 ±0.164	0.02325 ±0.00037	3.2403 ±0.0172	43	0.732	

2:15A, 2:21B, 1:156B, 2:81B and 2:89A) and two long-period SB2 (1:130A and 2:87A). The remaining stars are a pulsating variable (2:5B), three stars for which we obtained too few measurements (2:24B, 1:90A, 2:62A) and two stars that are probably not variable (2:91B and 2:99B). These objects are discussed in the notes in Section 4.4.

The average velocities of these stars, given in Table 3, are derived from the CORAVEL measurements only, since the offset between CORAVEL and another system like SOPHIE cannot be computed. Moreover, for the SB2 only the blended measurements are taken into account. The estimation of the uncertainty of the systemic RV is puzzling, since we do not even know when the range of RV variations was entirely covered by our measurements. As a consequence, and unlike the case of a constant star, the actual error in \bar{V} does not vary as the square root of the number of the measurements. Therefore, we finally chose to assume as error the standard deviation of the RV measurements.

4.4 Notes on individual objects

2:5A = BD +45 172. Four SOPHIE measurements were taken into account for each component. A correction of 3 m s⁻¹ was added to our original estimation of the RV calculated by fitting two Gaussian curves to the SOPHIE CCF.

2:5B = BD +45 171. The star is a semi-regular pulsating variable and the RV variations are probably not due to orbital motion.

2:8B = BD -01 133. This star was suspected to be a long-period SB1 on the basis of the CORAVEL measurements. However, the SOPHIE measurements do not confirm this hypothesis and their variations suggest a short period with a small amplitude.

1:18A = HD 8624. Revision of the orbit of Tokovinin (1999). Tokovinin's measurements were taken into account with a correction of +310 m s⁻¹, corresponding to the best fit.

2:13A = BD +10 303. Preliminary orbit; our observations cover only 79.5 per cent of the period.

2:14A = HD 13904. After increasing along the CORAVEL observations, the RV is slowly decreasing over our six SOPHIE measurements, confirming a long-period binary. Assuming a null offset between CORAVEL and SOPHIE, one obtains a possible period of 8000 d and a periastron around $T = 245\,3000$.

2:15A = BD +28 387s. The CORAVEL measurements suggest a long period and the average velocity of the SOPHIE measurements confirms this hypothesis. A very preliminary orbit was thus derived, with $P = (8000 \pm 2700)$ d, $T_0 = 244\,8000 \pm 800$ JD, $e = 0.3 \pm 0.1$, $V_0 = (8.8 \pm 0.4)$ km s⁻¹ and $K_1 = (1.3 \pm 0.3)$ km s⁻¹, but it does not look reliable, since the period is very uncertain. However, our three SOPHIE measurements exhibit variations that suggest the system could include a short-period component.

2:16A = HD 14446. The SB1 orbit was computed discarding all the measurements between 0 and -10 km s⁻¹, which seem to refer to a third component with fixed velocity. The measurements of the secondary component are not symmetric to those of the primary and

it is impossible to derive a SB2 orbit. Finally, part of a long-period orbit is visible in the large residuals of the SB1 orbit. Therefore, the system could be quadruple, although the CCF of a sole SOPHIE spectrum exhibits one dip only.

2:20B = BD +17 493p. Orbit calculated discarding the four blended measurements. When they are taken into account, the blend coefficient is $C_0 = 0.624 \pm 0.042$ but the orbital elements are not improved.

2:21B = BD +20 511. The SOPHIE measurements confirm the variability of the RV. A possible orbit was found with the following elements: $P = (3070 \pm 125)$ d, $T_0 = 244\,6400 \pm 300$ JD, $e = 0.5 \pm 0.3$, $V_0 = (26.7 \pm 0.5)$ km s⁻¹ and $K_1 = (4.8 \pm 1.8)$ km s⁻¹, but it is very uncertain due to the large errors of the CORAVEL measurements.

2:24B = HD 23158. A F5 V type star rather difficult to measure with CORAVEL, with very large uncertainties ($I = 2.7$ km s⁻¹). The possible variability is due to the measurement of JD 244 8245; when it is discarded, $P(\chi^2) = 12.2$ per cent. Therefore, the variability of the star is not certain. If it is constant, the RV of the star is $\bar{V} = (-1.95 \pm 1.81)$ km s⁻¹.

2:33A = HD 27635. The eight measurements of the secondary seem fixed around -28 km s⁻¹ and we prefer to discard them. Otherwise, a SB2 orbit is obtained with $K_2 = 8.3$ km s⁻¹.

2:38B = HD 285970. A first orbit was published by Griffin & Gunn (1981).

2:40A = HD 33185. A bright SB2 (6.67 mag) with a semi-major axis expected around 58 mas, which should be easily separated.

2:48B = HD 59450. The star belongs to a triple CPM system and is also 2:49A.

2:54B = HD 80101 = ADS 7288AB. A visual binary system with separation 0.3 arcsec. The A component is the SB1 with orbital elements in Table 4. The dip of the B component is visible in nine CORAVEL CCF, with the fixed velocity $V_B = (52.08 \pm 0.33)$ km s⁻¹. 29 blended RV refer to components A and B.

1:112A = HD 81997. Revision of the orbit of Duquennoy & Mayor (1991).

2:58B = HD 89745. A correction of 0.489 km s⁻¹ was added to the seven RV measurements derived from SOPHIE for each component, in order to get the best fit.

1:130A = HD 92787. A F5 star with large RV errors. A possible secondary component was detected on one correlation dip and it is possible that the other measurements contain blended observations.

1:130B = HD 92855. Revision of the orbit of Tokovinin (1994), which was based on 17 recent measurements but also on nine measurements performed between 1916 and 1932 (Abt 1970). We applied a correction of $+0.381$ km s⁻¹ for the former and $+1.45$ km s⁻¹ for the latter.

2:64B = BD +12 2343. A first orbit was published by Jeffries, Bertram & Spurgeon (1995).

1:156A = HD 102509. Orbit of Griffin & Griffin (2004), partly based on our RV measurements. The periastron epoch was converted in JD and the systemic velocity was translated in the CORAVEL system.

1:156B = BD +21 2357. Drift; the RV decreased over 10 yr.

2:68B = BD +28 2103. Revision of the orbit of Latham et al. (2002); we found a correction of -0.120 km s⁻¹ to apply to their measurements.

2:72A = HD 110025. A secondary dip was observed by Halbwachs et al. (2011), leading to the mass ratio $q \approx 0.64$.

2:72B = BD +17 2512. A secondary dip was observed by Halbwachs et al. (2011), leading to the mass ratio $q \approx 0.66$.

2:73B = HD 110106. A secondary dip was observed by Halbwachs et al. (2011), leading to the mass ratio $q \approx 0.75$.

1:175A = HD 112033. The star is ADS 8695, a visual binary with $P = 359$ yr, $a = 1.18$ arcsec and $\Delta m = 2.2$ mag (Heintz 1997); the secondary component is not visible on our observations and the SB1 orbit refers to the brightest component of the visual binary. A correction of -0.263 km s⁻¹ was applied to the seven original SOPHIE measurements.

2:81B = HD 234054. A SB1 observed over 11 years, but with a period still longer.

2:87A = HD 126661. The RV slightly decreases over 6600 d, until the two dips are separated in our last observations.

2:89A = HD 135117. A SB1 observed over 20 yr but with a period still longer.

2:91B = HD 150631. The variability status is questionable, since $P(\chi^2) = 1.5$ per cent when the measurement of JD 244 9931 is discarded. The RV is then (-12.0 ± 1.2) km s⁻¹.

2:92A = HD 153252. A G5-type star without luminosity class. Due to the short period, it cannot be a giant; assuming the primary component is a dwarf, the secondary component has a minimum mass around 50 Jupiter masses and it is a brown dwarf candidate.

2:97B = HD 164025. Orbit of Griffin (2003), partly based on our RV measurements. The periastron epoch was converted in JD, and the systemic velocity was translated in the CORAVEL system.

2:98B = HD 238865. The star is a triple system, consisting of a long-period SB1 with an additional short-period orbit. Preliminary elements of the short-period orbit were published by Tokovinin & Smekhov (1995); in order to avoid the drift due to the long period we rejected 21 of our CORAVEL measurements made before JD 244 9000 but took into account 16 measurements performed with Russian telescopes; the correction to add to the latter is $+1.15$ km s⁻¹.

2:99A = HD 169822. Revision of the orbit of Latham et al. (2002), with a correction of -0.328 km s⁻¹ to their measurements. The spectral type of the star is G7 V, leading to a minimum mass of around 30 Jupiter masses for the secondary component.

2:99B = HD 169889. This star was observed as G141-9 by Latham et al. (2002), who concluded it had a constant RV. A null value of $P(\chi^2)$ was obtained from all 10 CORAVEL measurements and also from the 11 SOPHIE measurements. Nevertheless, when one outlying measurement is discarded in both sets, $P(\chi^2)$ becomes 0.47 and 0.81, respectively. We conclude then that the RV is probably constant. The RV of the star is then $\bar{V} = (-18.139 \pm 0.114)$ km s⁻¹.

1:280A = HD 194765. A bright SB2 (6.70 mag) with a semi-major axis expected around 17 mas, which should be easily separated.

1:307A = HD 214511 = ADS 16111AB. Triple system already studied by Tokovinin (1998). A triple-system solution was computed, combining a long-period SB2 with a SB1 as primary component. The period of the SB2 was fixed to the value obtained by Docobo & Costa (1986) for a visual orbit, as reported in the Sixth Catalog of Orbits of Visual Binary Stars,¹ distributed by Mason & Hartkopf (2006). The assignment of the ‘c’ component index in Table 1 was carried out as follows: when only one RV was obtained it was assumed to be a blend as soon as the difference $|V_1 - V_2|$ was found to be less than 30 km s⁻¹. The solution presented in Table 6 is based on our measurements only, since it is better than the one obtained when the measurements of Tokovinin (1998) are added.

¹ <http://ad.usno.navy.mil/wds/orb6.html>.

5 CONCLUSION

An observational programme initiated to search for common RV stars among CPM stars resulted in the selection of 66 stars suspected to be variable. Thanks to observing runs distributed over a very long time (more than 20 years for 11 stars), we finally derived a first SB orbit for 40 stars. One of these orbits (2:92A=HD 153252) corresponds to a possible brown dwarf companion with a minimum mass equal to 50 Jupiter masses. We derive the elements of 13 SB2 orbits, assuming that the RV of the blended measurements are linear combinations of the RV of the components.

The periods of the 40 new orbits are on average rather long: more than 1 year for 20 stars, including five SB2, while three stars (1 SB2) even have periods between 10 years and around 15 years. Some of these binaries could be resolved and the masses of the components could be derived from the combination of the visual and spectroscopic observations. Among the SB2 brighter than 7 mag, two are ideal targets for speckle interferometry: 2:40A and 1:280A should have semi-major axes of 58 and 17 mas, respectively. Accurate masses should also be obtained in future, thanks to the astrometric orbits expected from the forthcoming *Gaia* mission (Halbwachs & Arenou 2009). For that purpose, seven new SB presented in that paper have now been measured with SOPHIE in order to improve their orbits.

In addition to the 40 new SB, we improved the orbital elements of 10 others. We also found 11 long-period SB, including two SB2, for which it was not possible to derive the orbital elements.

We are now able to select a sample of physical wide binaries, including components that are themselves close binaries, and to investigate the statistical properties of these stars and their relations with the other components of the Galaxy. This will be the topic of a forthcoming second paper.

ACKNOWLEDGMENTS

We have benefited during the entire period of these observations from the support of the Swiss National Foundation and Geneva University. We are particularly grateful to our technicians Bernard Tartarat, Emile Ischi and Charles Maire for their dedication to that experiment for more than 20 years. The SOPHIE observations were made thanks to a time allocation of the French Programme National de Physique Stellaire (PNPS); it is a pleasure to thank the OHP staff, and especially Mira Véron, for organizing these observations in service mode. We are grateful to Andrei Tokovinin for providing an additional RV measurement. We enjoyed discussion of the method for taking into account the blended measurements of SB2 with Frédéric Arenou. Joseph Lanoux and Audrey Morgenthaler made a preliminary calculation of the SB orbital elements. An anonymous referee made relevant comments, including several corrections of the English. Rodrigo Ibata carried out a last reading of the text, adding a few further improvements. We made use of Simbad, the data base of the Centre de Données astronomiques de Strasbourg (CDS).

This paper was based on observations performed at the Observatoire de Haute-Provence (CNRS), France.

REFERENCES

- Abt H. A., 1970, *ApJS*, 19, 387
 Baranne A., Mayor M., Poncet J.-L., 1979, *Vistas Astron.*, 23, 279
 Boisse I. et al., 2010, *A&A*, 523, A88
 Bouchy F. et al., 2009, *A&A*, 505, 853
 Duquenooy A., 1987, *A&A*, 178, 114
 Duquenooy A., Mayor M., 1991, *A&A*, 248, 485
 Docobo J. A., Costa J. M., 1986, *IAU Double Star Inf. Circ.* 99
 Griffin R., 2003, *The Observatory*, 124, 190
 Griffin R. F., Gunn J. E., 1981, *AJ*, 86, 588
 Griffin R. E. M., Griffin R. F., 2004, *MNRAS*, 350, 685
 Halbwachs J.-L., 1986, *A&AS*, 66, 131
 Halbwachs J.-L., Arenou F., 2009, in Heydary-Malayeri M., Reylé C., Samadi R., eds, *Proceedings SF2A 2009 – Scientific Highlights*, <http://www.sf2a.asso.fr/>, p. 35
 Halbwachs J.-L., Mayor M., Udry S., Arenou F., 2003, *A&A*, 397, 159
 Halbwachs J.-L., Arenou F., Famaey B., Guillout P., LEBRETON Y., Pourbaix D., 2011, in Alecian G., Belkacem K., Collin S., Samadi R., Valls-Gabaud D., eds, *Proceedings SF2A 2011 – Scientific Highlights*, <http://www.sf2a.asso.fr/>, p. 303
 Heintz W. D., 1997, *ApJS*, 111, 335
 Jeffries R. D., Bertram D., Spurgeon B. R., 1995, *MNRAS*, 276, 397
 Jiang Y.-F., Tremaine S., 2010, *MNRAS*, 401, 977
 Lacroute P., Valbousquet A., 1974, *A&AS*, 16, 343
 Latham D. W., Stefanik R. P., Torres G., Davis R. J., Mazeh T., Carney B. W., Laird J. B., Morse J. A., 2002, *AJ*, 124, 1144
 Luyten W. J., 1940, *Publ. Astron. Obs. Univ. Minnesota Vol. III*, 3, 35
 Luyten W. J., 1987, *Proper motion survey with the 48-inch Schmidt telescopes*, LXXI. Univ. Minnesota, Minnesota
 Mason B. D., Hartkopf W. I., 2006, *J. Double Star Obs.*, 2, 171
 Perruchot S. et al., 2008, *Proc. SPIE*, 7014, 17
 Pourbaix D. et al., 2004, *A&A*, 424, 727
 Struve F. G. W., 1852, in *Stellarum fixarum imprimis duplicium et multiplicium positiones mediae*. Academia. Caesare Petropolitanae, Saint-Petersbourg
 Tokovinin A. A., 1994, *Astron. Lett.*, 20, 717
 Tokovinin A. A., 1998, *Astron. Lett.*, 24, 288
 Tokovinin A. A., 1999, *A&AS*, 136, 373
 Tokovinin A. A., Smekhov M. G., 1995, *Astron. Lett.*, 21, 247

SUPPORTING INFORMATION

Additional Supporting Information may be found in the online version of this article:

Table 1–2. The full radial velocity catalogue, as described in Tables 1 and 2 (one file).

Phase plots. The phase plots of 49 systems, including a triple (50 figures).

Drift plots. Radial velocities as functions of epoch (17 figures).

Please note: Wiley-Blackwell are not responsible for the content or functionality of any supporting materials supplied by the authors. Any queries (other than missing material) should be directed to the corresponding author for the article.

This paper has been typeset from a $\text{\TeX}/\text{\LaTeX}$ file prepared by the author.